Mechanism of the Meerwein−Ponndorf−Verley−Oppenauer (MPVO) Redox Equilibrium on Sn− and Zr−Beta Zeolite Catalysts

Mercedes Boronat, Avelino Corma,* and Michael Renz

Instituto de Tecnología Química, UPV-CSIC, Universidad Politécnica de Valencia, Avenida de los Naranjos, s/n, 46022 Valencia, Spain

Received: May 26, 2006; In Final Form: July 27, 2006

The mechanism of the Meerwein−Ponndorf−Verley (MPV) reduction of cyclohexanone with 2-butanol catalyzed by Sn−beta and Zr−beta zeolites has been theoretically investigated using density functional theory (DFT) and the cluster approach. An experimental catalytic study has shown that the active sites in the MPV reaction catalyzed by Sn−beta are the same partially hydrolyzed Sn−OH groups that were found to be active for the Baeyer−Villiger (BV) reaction. The computational study indicates that the mechanism of Sn−beta and Zr−beta catalysis is similar, and involves the following steps: adsorption of both the ketone and the alcohol on the Lewis acid center, deprotonation of the alcohol, carbon-to-carbon hydride transfer, proton transfer from the catalyst, and products exchange. As in the aluminum alkoxide catalyzed reaction, the hydride shift occurs through a six-membered transition state, and the role of the hydrolyzed and therefore more flexible M−OH bond is just to facilitate the initial deprotonation of the alcohol.

1. Introduction

The Meerwein−Ponndorf−Verley (MPV) reduction of aldehydes and ketones and the complementary Oppenauer oxidation of alcohols (MPVO) are useful tools in organic synthesis, since they are chemoselective reactions that can be performed under mild conditions. Using secondary alcohols as hydrogen donors in the MPV reduction, carbonyl groups are selectively reduced in the presence of other reducible groups such as unsaturated C=C bonds, C−halogen bonds, or nitro groups. Thus, for example, α,β-unsaturated alcohols, which are important starting materials for the production of fine chemicals, can be easily obtained. The choice of the secondary reductant alcohol and the use of additional ligands influence regio-, stereo-, and enantioselectivities.[1,2]

The first promoters used in MPVO reactions were aluminum alkoxides, but they present the disadvantage that, due to difficulties during the ligand exchange step, stoichiometric amounts of the alkoxide are often needed. Higher reactivities have been achieved with dinuclear Al(III) complexes,[3] with Al(III) alkoxides generated in situ,[4] or with the introduction of Ln(III) alkoxides,[5] which can be used in catalytic amounts (5−10 mol %). The zirconium complex bis(cyclopentadienyl)-zirconium dihydride[6] and its hafnium analogue[7] have also been reported to be active in the MPV reaction.

To overcome some of the disadvantages of homogeneous catalysts, such as water sensitivity and catalyst separation, heterogeneous catalysts have been developed for the MPVO reactions. Metal oxides such as MgO,[8] γ-Al_2O_3,[9] and ZrO_2,[10] grafted alkoxides or alkyl complexes,[11−13] and zeolites[14−18] have also been successfully applied in the MPVO reactions of a number of ketones and alcohols. The best heterogeneous materials found up to now are zeolites containing well-defined and isolated Lewis acid centers, such as Sn- or Zr-substituted zeolites.[17,18]

In the first version of the MPV reduction with aluminum isopropoxide, the mechanism was supposed to proceed through a six-membered cyclic transition state in which both the ketone and the deprotonated alcohol are coordinated to the metal center of the metal alkoxide. The coordination of the ketone or aldehyde to the metal atom polarizes and activates the carbonyl double bond, facilitating the hydride shift from the alcoholate. In 1953 it was shown by deuterium tracer studies that the mechanism of Al(III) isopropoxide promoted reactions proceeds exclusively by a carbon-to-carbon hydrogen transfer.[19] More recent mechanistic studies using deuterium-substituted alcohols and catalysts[20] have confirmed the same carbon-to-carbon hydrogen transfer pathway for the MPVO reactions catalyzed by La(III) alkoxides, while in the case of Al−beta zeolite catalyst the reaction path depends on the substrate used. In a computational study of the reduction of acetophenone catalyzed by Al(III) complexes,[21] several reaction pathways were investigated and it was concluded that the classical and concerted direct hydrogen transfer mechanism is more favorable than either a stepwise hydridic route or a radical mechanism.

With respect to the mechanism of the MPVO reactions catalyzed by Sn- or Zr-substituted zeolites, no information can be found in the literature. Sn−beta zeolite is a highly active and selective catalyst for a number of Lewis acid catalyzed redox reactions, such as the MPV reduction of ketones and aldehydes,[22] the Baeyer−Villiger (BV) oxidation of carbonyl compounds with H_2O_2,[23] or the cyclization of citronellal to isopulegol,[24] while Zr−beta has been reported to show excellent activity and selectivity in the MPVO reactions of several substrates[25] and in the cyclization of citronellal to isopulegol.[26] The nature of the active sites in Sn−beta has been experimentally and theoretically investigated,[27,28] and it has been found that the activity of this catalyst for the Baeyer−Villiger oxidation of ketones with H_2O_2 is related to the presence of tetrahedrally coordinated framework tin atoms having one Sn−O−Si bond. These sites are bifunctional, and consist of the Lewis acidic tin atom that activates the carbonyl group and the adjacent basic

* Corresponding author. Fax: 34(96)3877809. E-mail: acorma@itq.upv.es.

10.1021/jp063249x CCC: $33.50
Published on Web 09/22/2006

oxygen atom of the Sn−OH group, which is able to form a hydrogen bond with H_2O_2. If the same bifunctional sites were the active centers in the MPV reduction of carbonyl compounds catalyzed by Sn−beta zeolite, besides the classical mechanism involving a hydride shift between the ketone and the alcoholate coordinated to the metal center, the reductant alcohol molecule could form a hydrogen bond with the basic oxygen atom and the reaction could proceed without deprotonation of the alcohol, following a reaction path different from that proposed for the Al(III) catalyzed reactions.

We present in this work a complete computational study of the mechanism of the MPV reduction of cyclohexanone with 2-butanol catalyzed by Sn−beta and Zr−beta zeolites. Several possibilities for adsorption of cyclohexanone and 2-butanol on the Lewis acid active site have been considered, and the different reaction paths starting from these adsorption complexes have been investigated. Moreover, an experimental catalytic study has been performed in order to clarify (a) whether the active sites for the Sn−beta catalyzed MPV reaction are the same partially hydrolyzed Sn−OH groups that were found active for the BV reaction, (b) whether the mechanism involves an alcoholate intermediate formed by deprotonation of the alcohol as in Al(III) and La(III) catalyzed reactions, and (c) which are the catalytic differences between Sn−beta and Zr−beta for the MPV reaction.

2. Experimental Methods

2.1. Computational Details. Previous computational and spectroscopic work[27,28] showed that the catalytic activity of Sn−beta zeolite for the Baeyer−Villiger oxidation of ketones with H_2O_2 is related to the presence of tetrahedrally coordinated framework tin atoms having one hydrolyzed Sn−O−Si bond. As it will be discussed later, framework Sn and Zr centers are responsible for the catalytic activity in the Meerwein−Ponndorf−Verley reaction, and therefore Sn(O−SiH_3)$_3$OH and Zr(O−SiH_3)$_3$OH clusters of atoms were used to simulate the Lewis acid active sites. To build these models, in a first step a cluster of atoms containing four coordination spheres around the T9 position was cut out from the periodic structure of pure silica beta zeolite[29] (see Figure 1), the central Si atom was substituted by a metal atom M (M = Sn, Zr), and one of the M−O−Si(−O)$_3$ groups was substituted by a M−O−H group. The dangling bonds that connected the cluster to the rest of the solid were saturated with H atoms at 1.49 Å from the Si atoms and oriented toward the positions occupied in the crystal by the oxygen atoms in the next coordination sphere, and the geometry of the two resulting structures was optimized by means of the ONIOM scheme[30,31] as implemented in the Gaussian03 computer program.[32] The ONIOM approach subdivides the *real* system into a *model* system, which is described at the highest level of theory, and subsequent parts or layers that are computed at progressively lower and computationally cheaper levels of theory. In this work, the model system includes the M atom, the four oxygen atoms in the first coordination sphere, and the Si or H atoms bound to them. The coordinates of these atoms were completely optimized with the density functional B3PW91 method[33,34] using a LANL2DZ effective core potential basis set for Zr[35] and Sn,[36] and the standard 6-31G(d,p) basis set[37] for O, Si, and H atoms. The rest of the system was treated at the HF/3-21G level of theory, and only the coordinates of the terminal H atoms were kept fixed at their original positions. The combination of levels of theory (DFT/DZP:HF/3-21G) and the size of the model system chosen for the ONIOM calculations have been reported to provide results in excellent agreement with those obtained with full DFT periodic calculations.[38] The optimized values of the four Sn−O and four Zr−O distances in the large clusters are on average 1.881 and 1.963 Å, respectively, reflecting the size of the incorporated metal atom.

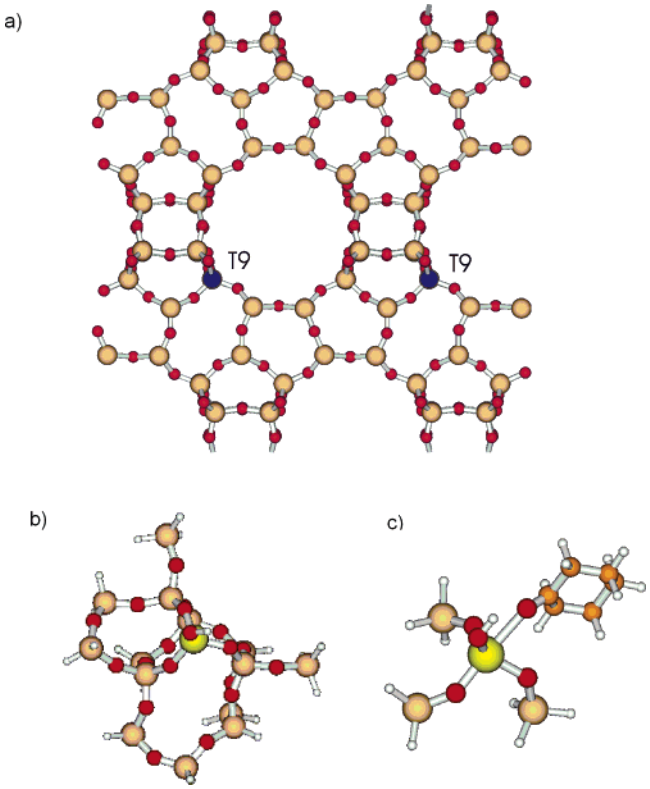

Figure 1. (a) Topology of beta zeolite showing T9 position. (b) Large cluster and (c) small cluster with adsorbed cyclohexanone (**A0**).

In a second step, the smaller Sn(O−SiH_3)$_3$OH and Zr(O−SiH_3)$_3$OH clusters used to calculate the reaction mechanism were cut out from the optimized structures of these large models. Again, the dangling bonds that connected the small cluster to the rest of the solid were saturated with H atoms at 1.49 Å from the Si atoms. The computational study of the reaction mechanism was performed at the B3PW91/LANL2DZ,6-31G(d,p) level, and in all the minima and transition state geometry optimizations the coordinates of the organic molecules, the M, O, and Si atoms, and the H of the M−O−H group were set completely free, while the H terminations of the Si atoms were kept fixed at their original positions. The nature of every stationary point was characterized by means of frequency calculations and analysis of the vibrational modes, and all calculated energies were corrected for the zero-point vibrational energies (ZPE). Orbital energies and occupancies and atomic charges were obtained with natural bond orbital (NBO) methods.[39]

It should be pointed out that the T9 position was chosen because a preliminary molecular mechanics study[28] of Sn location in BEA zeolite indicated that this was the most favorable position for Si → Sn substitution. More recently, two different periodic DFT studies found either no preferential location for Sn[40] or preferential occupation of the T2 position[41] in BEA zeolite. Since the optimized structural parameters reported in the more complete computational study of Pal et al.[41] indicate that the deformation of the framework caused by Sn incorporation is quite localized and similar in all nine positions, and in this work the local geometry around the metal center is fully optimized, we can assume that the MPV reaction mechanism calculated is valid for all possible locations of Sn.

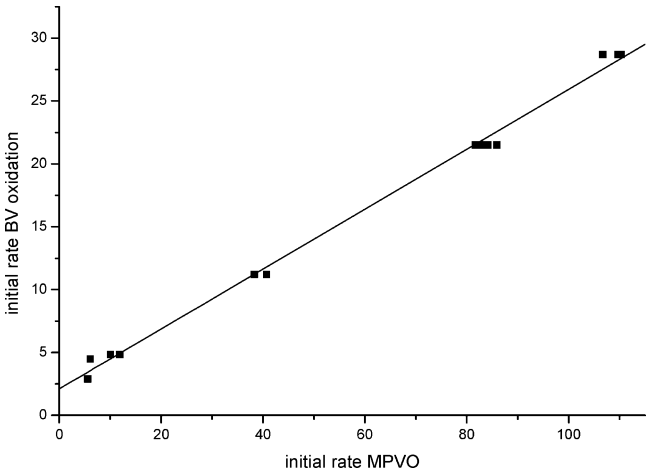

Figure 2. Correlation of initial rate of the Baeyer−Villiger oxidation of adamantanone with H_2O_2 (in mmol/h/g of catalyst) versus initial rate of the Meerwein−Ponndorf−Verley reduction of cyclohexanone with 2-butanol. Both reactions were catalyzed by a series of samples of Sn−beta zeolite subjected to different postsynthesis treatments.

2.2. Catalyst Preparation. The beta catalysts were prepared in fluoride media following literature procedures[23,25] and were calcined at 853 K for 3 h. The zeolites showed high crystallinity, and no peaks of SnO_2 or ZrO_2 were found by X-ray diffraction (XRD). Nitrogen adsorption experiments on the calcined beta samples gave an isotherm very similar to that of pure silica beta with a micropore volume of 0.21 $cm^3\ g^{-1}$ and BET surface areas of 450−475 $m^2\ g^{-1}$. The metal content was determined by atomic absorption and the following silicon−metal ratios were obtained: Si/Sn = 108 and Si/Zr = 116.

2.3. Catalytic Reactions. *Baeyer−Villiger Oxidations (BV).* A 500-mg sample of adamantanone was mixed with 500 mg of 35% aqueous hydrogen peroxide and 3.0 g of dioxane. A 50-mg sample of the catalyst was added, and the reaction mixture was stirred and heated to 90 °C for 7 h. The progress of the reaction was monitored by gas chromatography (HP-5 column, 15 m, 0.32 mm, 0.5 μm with an adequate temperature program). The initial rates were calculated after 30 and 180 min reaction time for Sn−beta and Zr−beta, respectively.

Meerwein−Ponndorf−Verley Reductions (MPV). A stock solution of 855 mg of cyclohexanone and 33.36 g of 2-butanol was prepared. A 3.42-g sample of this stock solution was placed in a round-bottom flask, and a 7.5-mg sample of the catalyst was added. The reaction mixture was stirred and heated to 100 °C for 1 h. The progress of the reaction was monitored by gas chromatography (HP-5 column, 15 m, 0.32 mm, 0.5 μm with an adequate temperature program). The initial rates were calculated after 5 and 15 min reaction time for Sn−beta and Zr−beta, respectively.

3. Results and Discussion

3.1. Catalytic Activity Measurements. It is known from previous work[27] that the catalytic activity of Sn−beta for the BV reaction directly correlates with the concentration of partially hydrolyzed framework Sn−OH sites, and that catalysts with different concentrations of these sites can be obtained by modifications in the calcination procedure. A series of Sn−beta samples subjected to different postsynthesis treatments, and therefore containing different numbers of partially hydrolyzed Sn−OH sites, were used to catalyze the BV oxidation of adamantanone with H_2O_2 and the MPV reduction of cyclohexanone with 2-butanol, and the initial rates for both reactions were measured and compared (see Figure 2). There is a linear relationship between both series of data that meets the origin, indicating that the BV and the MPV reactions are catalyzed by the same type of center, i.e., the partially hydrolyzed framework Sn−OH group. As previously explained, this active site is bifunctional and consists of a Lewis acid tin atom to which both cyclohexanone and 2-butanol can coordinate, and the adjacent basic oxygen atom able to form a hydrogen bond with the alcohol.

3.2. Reaction Mechanisms with Sn−Beta. A very particular characteristic of the MPVO reactions is that a carbonyl compound is reduced to an alcohol molecule while an alcohol is oxidized to the corresponding carbonyl compound; i.e., the oxidation reaction is exactly the inverse of the reduction reaction and the sum of carbonyl compounds and of alcohols is the same before and after the hydride shift. If the reaction is really catalytic, i.e., the catalyst is provided only in catalytic amounts and remains unchanged after the reaction, and the carbonyl compound does not involve any kind of extra stabilization (as in a conjugated double bond), the system cannot differentiate substrates and products. There is no real driving force and the reaction system will tend to a statistical equilibrium. Consequently, in the computational study we have considered all the possible types of complexes that can be formed by interaction of one carbonyl compound and one alcohol molecule with the catalyst active site, and we have searched for transition states connecting these minima.

There are five different ways in which cyclohexanone and 2-butanol can adsorb on the Sn−beta active site without deprotonation (structures **A1**−**A5** in Chart 1) and five corresponding structures **A1′**−**A5′** (not depicted) with interchanged carbon skeletons, that is, with cyclohexanol and 2-butanone adsorbed on the active site. Since the interactions in every pair of complexes **A**−**A′** are the same, their energies differ by less than ∼1 kcal/mol. There are also two complexes with the alcohol coordinated as alcoholate to the metal center, with the proton bound to the adjacent hydroxy group forming a water ligand, and with the ketone as additional adsorbate (structures **D1** and **D2** in Chart 1, and the corresponding **D1′** and **D2′** not depicted).

In structure **A1**, both the O_a atom of the ketone and the O_b atom of the alcohol are coordinated to the metal center. In **A2** and **A3**, cyclohexanone is also directly interacting with tin, but the alcohol is coordinated by hydrogen bonding either to the basic O_c atom (**A2**) or to the H_c proton (**A3**) of the Sn−OH group. In the two other adsorption complexes, the O_b atom of the alcohol is directly coordinated to the Sn atom, while the O_a atom of the carbonyl group is forming a hydrogen bond either with the H_c of the Sn−OH group as in **A4** or with the alcohol hydroxy H_a atom as in **A5**. The interaction of the metal center with the alcohol O_b seems to be slightly stronger than with the carbonyl O_a, since the calculated Sn−O_b distances are always shorter than the Sn−O_a values (see Table 1), and the most stable structures are **A1**, **A4**, and **A5**. The activation of the carbonyl group by the active site is also different in the five complexes considered. It is known[28] that the Lewis acid−base interaction of cyclohexanone with the Sn−beta active site involves not only the electron density transfer from the organic molecule to the catalyst, but also a back-donation from the catalyst to the antibonding π^*(CO) orbital of cyclohexanone. This back-donation causes a lengthening of the C_a−O_a bond reflected in a experimentally measured shift of the ν(CO) vibration frequency to lower values,[23] and an increase in the positive atomic charge on the C_a atom. Thus, while the C_a−O_a bond length calculated for one isolated cyclohexanone molecule at the B3PW91/6-31G(d,p) level of theory is 1.215 Å, the value

CHART 1

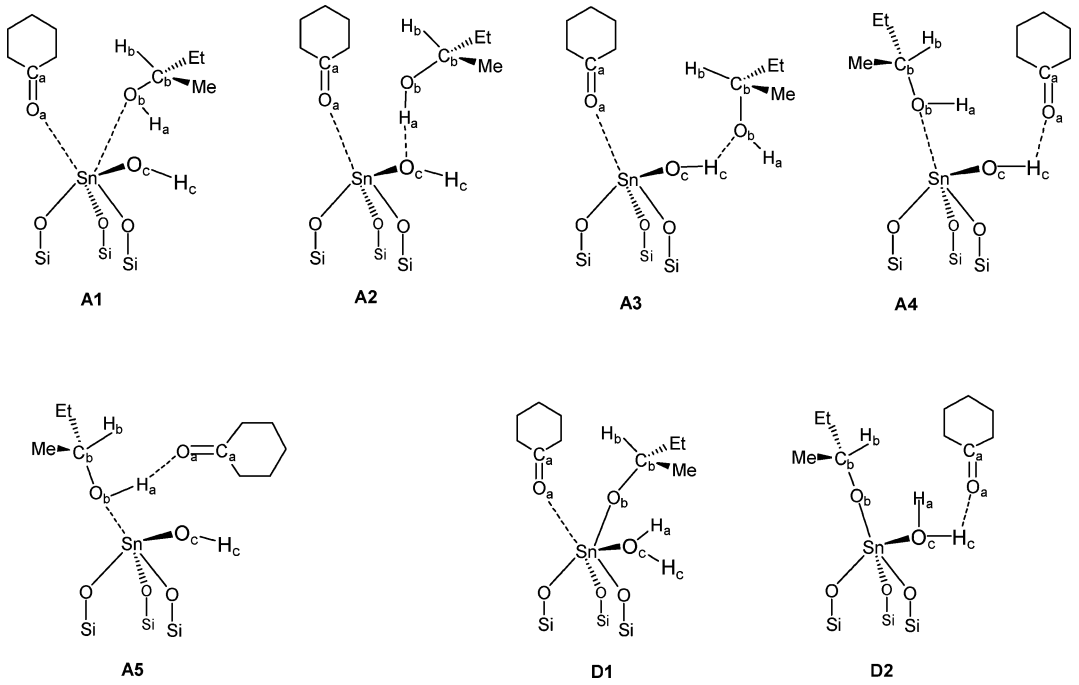

TABLE 1: Relative Energies (kcal/mol),[a] Optimized Bond Lengths (Å), Net Atomic Charge on the Carbonyl C_a Atom (*e*), and NBO Calculated Occupancy of the Cyclohexanone π^*(CO) Orbital (*e*) in the Different Adsorption Complexes Depicted in Chart 1

	E_{rel}	r(Sn−O_a)	r(Sn−O_b)	r(Sn−O_c)	r(C_a−O_a)	q(C_a)	occ π^*(CO)
A1	−19.6	2.325	2.247	1.954	1.233	0.666	0.113
A2	−15.7	2.269	3.865	1.942	1.234	0.672	0.117
A3	−18.9	2.297	3.629	1.904	1.232	0.669	0.113
A4	−19.6	4.090	2.288	1.919	1.222	0.619	0.092
A5	−21.1	4.238	2.200	1.930	1.227	0.638	0.101
D1	−16.4	2.356	1.979	2.299	1.232	0.665	0.118
D2	−20.9	4.488	1.935	2.275	1.226	0.628	0.098
A1−Zr	−26.2	2.387	2.343	2.045	1.227	0.660	0.110
D1−Zr	−26.0	2.417	2.037	2.416	1.233	0.670	0.120

[a] Calculated with respect to the sum of the energies of cyclohexanone + 2-butanol + the M(O−SiH_3)$_3$OH cluster model.

obtained for cyclohexanone adsorbed on the Sn(O−SiH_3)$_3$OH cluster model (structure **A0** in Figure 1c) is 1.230 Å, and the net atomic charge on C_a increases from 0.592 to 0.666 |*e*| by adsorption on the tin center. Subsequent adsorption of a 2-butanol molecule either on the tin center (**A1**) or by hydrogen bonding to the O_c−H_c group (**A2** and **A3**) enhances the activation of the carbonyl group, with the C_a−O_a bond lengths, the q(C_a) calculated values, and the occupancies of the π^*(CO) orbital in structures **A1**−**A3** being slightly larger than in the cyclohexanone adsorption complex **A0**. When cyclohexanone interacts with a proton as in structures **A4** and **A5**, the resulting system is more stable, but the shorter C_a−O_a bond lengths and the lower values obtained for q(C_a) and π^*(CO) occupancy indicate that the carbonyl group is less activated in these systems.

If the alcohol is deprotonated, the hydroxy proton H_b is transferred to the basic O_c atom of the Sn−OH group, and the resulting system can be described as a Sn alcoholate with a water molecule coordinated to the metal. The higher flexibility of the hydrolyzed Sn−O_c bond with respect to the other three Sn−O−Si bonds facilitates the process, allowing a lengthening of the Sn−O_c distance to ∼2.3 Å (see Table 1). There are only two different ways in which cyclohexanone can interact with this site: by direct coordination to the now less Lewis acidic metal center as in structure **D1**, or by hydrogen bonding to the water molecule as in **D2**. The activation of the carbonyl group in these two structures follows the trend observed in the nondeprotonated **A** systems: the activation of the CO bond is larger when cyclohexanone directly interacts with the Lewis acid tin center (structure **D1**).

Although **A5** is the most stable complex localized on the potential energy surface, the energy difference with respect to **A2**, which is the less stable, is only 5.4 kcal/mol, indicating that all seven systems are energetically accessible under reaction conditions. The transformation within the **A** series or from **D1** to **D2** and vive versa can be achieved by ketone desorption/adsorption involving low-energy barriers. The deprotonation of the alcohol occurs through a transition state in which the H_a atom is halfway between the alcohol O_b atom and the O_c atom of the Sn−OH group. It has been found that this deprotonation can only occur when the alcohol is directly coordinated to the metal center and H_a is not interacting with the carbonyl group. Two transition states of this type have been localized and are depicted in Chart 2: **TS1** connecting **A1** with **D1**, and **TS2** converting **A4** into **D2**. The activation energy calculated for the deprotonation of **A1** to give **D1** is 4.9 kcal/mol, while the barrier for the reverse process is lower, 1.7 kcal/mol. The activation energies involved in the **A4** → **D2** and **D2** → **A4** processes are slightly higher, 7.0 and 8.3 kcal/mol, respectively, but still allow us to conclude that all type **A** and type **D** complexes are energetically accessible during the reaction.

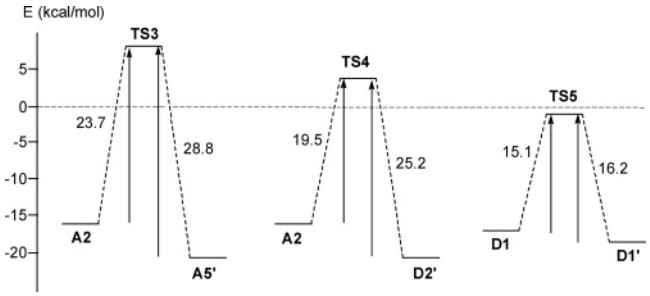

Figure 3. Calculated energy profiles for the three steps obtained that involve a change in the oxidation state of C_a and C_b carbon atoms.

CHART 2

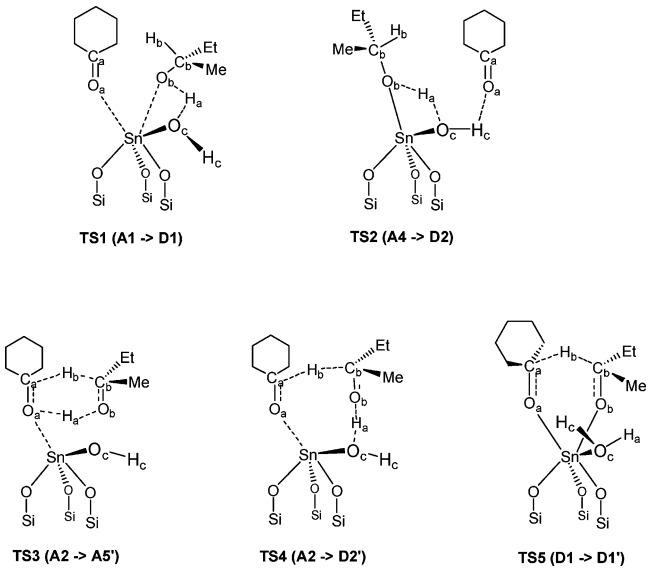

Three transition states were localized that involve a change in the oxidation state of the carbonyl carbon atom (C_a) and the carbon atom bearing the hydroxy group (C_b), i.e., that converted simultaneously cyclohexanone into cyclohexanol (or cyclohexanolate) and 2-butanol (or 2-butanolate) into 2-butanone (see Chart 2).

The first process considered occurs through the six-membered transition state **TS3**. Starting from complex **A2**, a simultaneous transfer of H_a to the carbonyl O_a atom and of H_b to the C_a atom gives as a result cyclohexanol coordinated to the Lewis acid Sn atom and 2-butanone forming a hydrogen bond with H_a (structure **A5′**). It can be seen in Table 2 that the C_a-H_b optimized distance in **TS3** is considerably shorter than the H_b-C_b value, and that the H_a atom is still covalently bonded to O_b, although strongly interacting with O_a. This indicates that the hydride shift is more advanced than the proton transfer. As shown in Figure 3, the activation barrier calculated for this process is high, 23.7 kcal/mol, and the reaction products are 5.1 kcal/mol more stable than the initial reactants. This pathway is very similar to the gas-phase mechanism; only one molecule is coordinated to the tin center and the capacity of the catalytic site is not fully exhausted. It should be mentioned that there is a corresponding pathway that converts structure **A5** into **A2′** through a similar transition state **TS3′**; however, it is not further considered because the activation barrier is higher, ∼30 kcal/mol, and the process is endothermic by ∼5 kcal/mol.

In the second pathway found, the initial complex is again **A2**, but during the reaction the H_a proton of the 2-butanol molecule is directly transferred not to the carbonyl O_a, but to the O_c atom of the Sn−OH group, giving as a result structure **D2′**. This occurs through the eight-membered transition state **TS4**, with an activation barrier of 19.5 kcal/mol. As in **TS3**, the hydride transfer from C_b to C_a is more advanced than the proton transfer from O_b to O_c, as indicated by the optimized geometry of **TS4** given in Table 2. The activation barrier for the reverse process, i.e., conversion of **D2′** into **A2**, is 25.2 kcal/mol, as a result of the higher stability of the alcoholate with respect to the adsorption complex.

The third transition state that involves a hydride transfer between C_a and C_b is **TS5**, which directly connects the deprotonated complex **D1** with the corresponding **D1′** system. Through this cyclic six-membered transition state, similar to that proposed for the Al alkoxide catalyzed reaction, H_b is transferred from C_b in the alcoholate to C_a in cyclohexanone, with an activation energy of 15.1 kcal/mol. In **TS5** the H_b atom is halfway between C_a and C_b, the $Sn-O_a$ and $Sn-O_b$ distances are similar and around 2.1 Å, and the C_a-O_a and C_b-O_b calculated bond lengths are intermediate between those corresponding to single and double C−O bonds. The hydride character of the transferring H_b atom is given by the net atomic charge on it, 0.18 *e*. Since the two minima connected by **TS5** are almost degenerate, the activation barriers for the direct and the reverse processes are similar, as shown in Figure 3. The relative energies of **TS3**, **TS4**, and **TS5** with respect to separated reactants are 8.0, 3.8, and −1.3 kcal/mol, respectively. These values are considerably higher than those calculated for **TS1** and **TS2**, confirming that the rate-determining step in the MPVO reaction is the hydride transfer between C_a and C_b. Comparison of the three calculated energy profiles depicted in Figure 3 indicates that the reaction occurs through **TS5**, following a mechanism similar to that described for the Al alkoxide catalyzed reaction.

The complete pathway is depicted in Figure 4 and consists of three steps: (1) deprotonation of **A1** into **D1** with an activation energy of 4.9 kcal/mol, (2) hydride transfer between **D1** and **D1′** with an activation barrier of 15.2 kcal/mol, and (3) conversion of **D1′** into **A1′** with an activation energy of only 2.0 kcal/mol.

TABLE 2: Optimized Distances (in Å) and Relative Energies (kcal/mol)[a] of the Transition States Depicted in Chart 2

	TS1	TS2	TS3	TS4	TS5	**TS1−Zr**	**TS5−Zr**
$r(Sn-O_a)$	2.301	4.205	2.168	2.039	2.094	2.407	2.204
$r(O_a-C_a)$	1.234	1.225	1.339	1.330	1.309	1.231	1.305
$r(C_a-H_b)$	5.328	7.191	1.272	1.237	1.363	5.808	1.371
$r(H_b-C_b)$	1.098	1.096	1.461	1.544	1.350	1.100	1.354
$r(C_b-O_b)$	1.439	1.434	1.312	1.293	1.312	1.421	1.304
$r(O_b-Sn)$	2.117	2.082	4.107	3.759	2.111	2.198	2.159
$r(O_b-H_a)$	1.241	1.192	1.055	1.063	2.074	1.203	2.808
$r(H_a-O_c)$	1.193	1.242	1.435[b]	1.401	0.973	1.220	0.965
$r(Sn-O_c)$	2.128	2.064	1.936	1.991	2.293	2.215	2.446
E_{rel}	−14.7	−12.6	8.0	3.8	−1.3	−22.2	−10.5

[a] Calculated with respect to the sum of the energies of cyclohexanone + 2-butanol + the $M(O-SiH_3)_3OH$ cluster model. [b] $r(H_a-O_a)$.

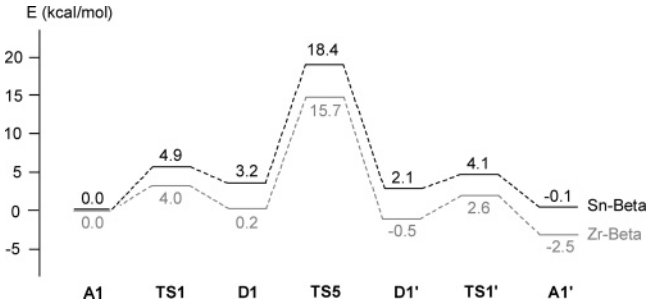

Figure 4. Calculated energy profiles for the Sn−beta and Zr−beta catalyzed reaction mechanisms.

3.3. Reaction Mechanisms with Zr−Beta. The detailed computational study of the potential energy surface of the Sn−beta catalyzed MPV reaction of cyclohexanone with 2-butanol indicates that the only reaction pathways that finally lead to a change in the oxidation states of C_a and C_b carbon atoms start either from **A1** or from **A2**, and that the deprotonated species **D2** is not involved in any of these mechanisms. Therefore, only adsorption complexes **A1** and **A2** and the deprotonated structure **D1** have been initially searched on the Zr−beta catalyzed potential energy surface. The optimized distances, relative energies, net atomic charge on the C_a atom, and calculated occupancies of the π^*(CO) orbital in structures **A1**−**Zr** and **D1**−**Zr** are listed in Table 1. The Zr−O optimized bond lengths are in all cases larger than the Sn−O values due to the larger size of the zirconium atom, but the degree of activation of the carbonyl group in **A1**−**Zr** and **D1**−**Zr** is similar to that in the corresponding structures of Sn−beta. However, it was not possible to find a minima corresponding to structure **A2**−**Zr**. The reason is the different natures of the lowest unoccupied molecular orbital (LUMO) in Sn−beta and of that in Zr−beta, depicted in Figure 5. The LUMO in the Sn−beta active site is a linear combination of the four antibonding σ^*(Sn−O) orbitals. When a Lewis base molecule such as cyclohexanone interacts with this site, the electron density transferred to the catalyst cannot be accepted by the tin atom, which pushes it into the orbital lobes located on the oxygen atoms. Thus, the oxygen atoms bonded to tin show a certain basic character and allow hydrogen bonding with the hydroxyl proton of 2-butanol. However, the LUMO in the Zr−beta catalyst is the d_{z^2} orbital on the zirconium atom, and it can accept the electron density transferred from the Lewis base molecule without increasing the basic character of the neighboring oxygen atoms.

SCHEME 1: Meerwein−Ponndorf−Verley Reduction of Cyclohexanone with 2-Butanol Catalyzed by Sn−Beta and Zr−Beta

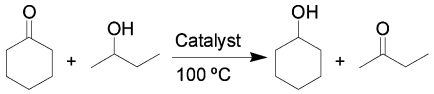

Catalyst	Ratio Si/M	initial rate [mmol/h/g cat]	TOF [mmol/mmol cat/h]
Sn-Beta	107	295	1940
Zr-Beta	116	65.6	465

Therefore, there is only one possible reaction path for the Zr−beta catalyzed MPV reduction of cyclohexanone with 2-butanol, equivalent to that obtained in the previous section for the Sn−beta catalyzed process (see Figure 4). In a first step, the adsorption complex **A1**−**Zr** is converted into the deprotonated species **D1**−**Zr** through the transition state **TS1**−**Zr** with an activation energy of 4.0 kcal/mol. The less basic character of the O_c atom bonded to Zr is reflected in the fact that, while in **TS1** the transferring H_a atom is closer to O_c than to O_b, in **TS1**−**Zr** the O_b−H_a distance is shorter than the H_a−O_c one (see Table 2). The rate-determining step is the hydride shift that converts **D1**−**Zr** into **D1′**−**Zr** through transition state **TS5**−**Zr**; the optimized geometry and the activation energy involved are similar to those obtained for the Sn−beta catalyzed process. Finally, **D1′**−**Zr** is converted into the product complex **A1′**−**Zr** through transition state **TS1′**−**Zr**. The calculated activation energy is low, 3.1 kcal/mol, and the step is exothermic by 2.0 kcal/mol.

Comparison of the energy profiles depicted in Figure 4 shows that the energy barrier for the rate-determining step is similar on both catalysts, suggesting that Zr−beta could also be a good catalyst for the MPV reaction. There is not much experimental information comparing the activity of both catalysts. In ref 25 it is reported that for the MPV reduction of 4-*tert*-butylcyclohexanone with 2-propanol the conversion over Sn−beta is similar to that over Zr−beta with high Si/Zr ratio, and increases with increasing Zr content. We have measured initial reaction rates and turnover frequency (TOF, mol of substrate converted per mol of catalytic sites and per hour) numbers for the MPV reduction of cyclohexanone with 2-butanol (see Scheme 1) and have found that Sn−beta is much more active than Zr−beta. It is worth mentioning that the TOF numbers given in Scheme 1 should be considered with care, because they have been calculated assuming that all Sn and Zr centers in the zeolite

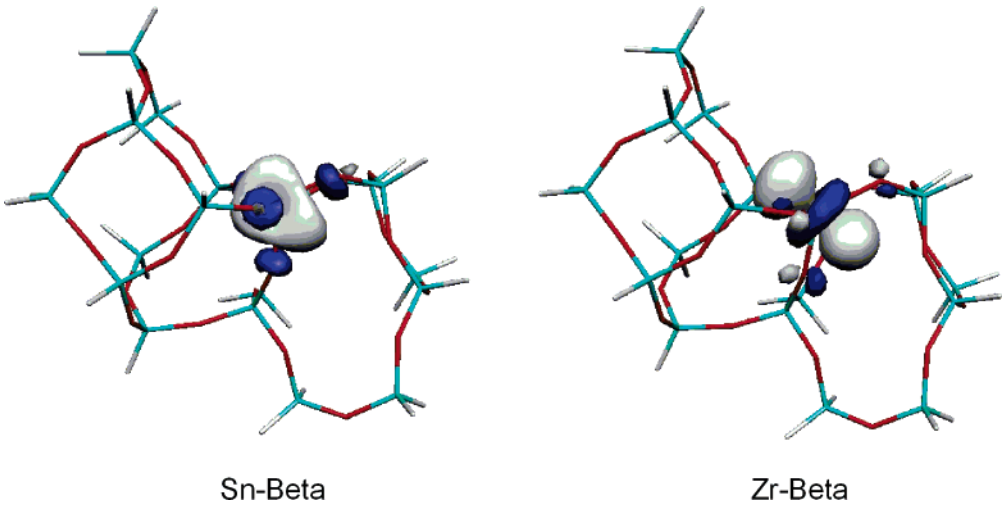

Figure 5. LUMO of Sn−beta and Zr−beta active sites.

samples are active. In the case of Sn−beta, it is known[27] that only about 20% of the tin centers are hydrolyzed, which means that the real TOF number for this catalyst would probably be even higher. However, we do not have any data concerning the number of hydrolyzed Zr sites in Zr−beta, and therefore we can only compare TOF numbers based on total metal content. Thus, taking this into account together with our theoretical calculations, we would predict that only about 5% of the total Zr in Zr−beta zeolite is active for this reaction. The rest of the Zr is either occupying extraframework positions or is incorporated into the framework forming nonhydrolyzed centers.

4. Conclusions

The mechanism of the MPV reduction of cyclohexanone with 2-butanol catalyzed by Sn−beta and Zr−beta zeolites has been theoretically investigated, and complementary catalytic activity tests have been performed to determine the nature of the Sn−beta active sites. Comparison of the initial rates measured for the Baeyer−Villiger oxidation of adamantanone with H_2O_2 and the MPV reduction of cyclohexanone with 2-butanol for a series of samples of Sn−beta catalysts subjected to different postsynthesis treatments shows that the active sites in the BV and MPV reactions are the same, i.e, the partially hydrolyzed framework Sn−OH sites.

The computational study shows that, among the seven different ways in which cyclohexanone and 2-butanol can adsorb on the bifunctional Sn−beta active site, only those in which the carbonyl group is directly coordinated to the Lewis acid metal center are able to activate the CO bond for the MPV reduction. The reaction pathway with the lowest activation energy, and therefore the most probable, is similar to that reported for the Al(III) and La(III) catalyzed reactions, and consists of three steps: (1) deprotonation of 2-butanol, (2) hydride shift through a six-membered cyclic transition state in which both the ketone and the deprotonated alcohol are directly bonded to the Sn atom, and (3) proton transfer from the catalyst to form cyclohexanol. The role of the hydrolyzed Sn−OH group in the MPV reaction is not to bind the alcohol molecule through hydrogen bonding as was the case for H_2O_2 in the BV reaction, but to allow the deprotonation of the alcohol to give an alcoholate intermediate bonded to the tin center and a water molecule.

The mechanism for the Zr−beta catalyzed reaction is equivalent to that found for Sn−beta and involves the same initial and intermediate species. The activation energy of the rate-determining step, i.e., the hydride transfer, is about 15 kcal/mol in both cases, and therefore it can be concluded, in agreement with experimental information, that both catalysts are active for the MPV reaction.

Acknowledgment. The authors thank CICYT (MAT-2006-3798164) for financial support and the Universitat de Valencia for computing facilities. M.R. is grateful to the Spanish Ministry of Science and Technology for a "Ramón y Cajal" fellowship.

References and Notes

(1) de Graauw, C. F.; Peters, J. A.; van Bekkum, H.; Huskens, J. *Synthesis* **1994**, 1007.

(2) Creyghton, E. J.; Huskens, J.; van der Waal, J. C.; van Bekkum, H. In *Heterogeneous Catalysis and Fine Chemicals IV*; Blaser, H. U., Baiker, A., Prins, R., Eds.; Elsevier: Amsterdam, 1997; p 531.

(3) Ooi, T.; Miura, T.; Itagaki, Y.; Ichikawa, H.; Maruoka, K. *Synthesis* **2002**, 279.

(4) Campbell, E. J.; Zhou, H.; Nguyen, S. T. *Org. Lett.* **2001**, *3*, 2391.

(5) Namy, J. L.; Souppe, J.; Collin, J.; Kagan, H. B. *J. Org. Chem.* **1984**, *49*, 2045.

(6) Ishii, Y.; Nakano, T.; Inada, A.; Kishigami, Y.; Sakurai, K.; Ogawa, M. *J. Org. Chem.* **1986**, *51*, 240.

(7) Nakano, T.; Umano, S.; Kino, Y.; Ishii, Y.; Ogawa, M. *J. Org. Chem.* **1988**, *53*, 3752.

(8) Kaspar, J.; Trovarelli, A.; Lenarda, M.; Graziani, M. *Tetrahedron Lett.* **1989**, *30*, 2705.

(9) Gargano, M.; D'Orazio, V.; Ravasio, N.; Ross, M. *J. Mol. Catal.* **1990**, *58*, L5.

(10) Kuno, H.; Takahashi, T.; Shibagaki, M.; Shimazaki, K.; Matsushita, H. *Bull. Chem. Soc. Jpn.* **1990**, *63*, 1943.

(11) Anwander, R.; Palm, C.; Gerstberger, G.; Groeger, O.; Engelhardt, G. *Chem. Commun.* **1998**, 1811.

(12) Zhu, Y.; Jaenicke, S.; Chuah, G. K. *J. Catal.* **2003**, *218*, 396.

(13) De Bruyn, M.; Limbourg, M.; Denayer, J.; Baron, G. V.; Parvulescu, V.; Grobet, P. J.; De Vos, D. E.; Jacobs, P. A. *Appl. Catal., A: Gen.* **2003**, *254*, 189.

(14) Creyghton, E. J.; Ganeshie, S. D.; Downing, R. S.; van Bekkum, H. *J. Mol. Catal. A: Chem.* **1997**, *115*, 457.

(15) van der Waal, J. C.; Kunkeler, P. J.; Tan, K.; van Bekkum, H. *J. Catal.* **1998**, *173*, 74.

(16) Corma, A.; Nemeth, L. T.; Renz, M.; Valencia, S. *Nature* **2001**, *412*, 423.

(17) Corma, A.; Domine, M. E.; Nemeth, L.; Valencia, S. *J. Am. Chem. Soc.* **2002**, *124*, 3194.

(18) Zhu, Y.; Jaenicke, S.; Chuah, G. K. *Chem. Commun.* **2003**, 2734.

(19) Williams, E. D.; Krieger, K. A.; Day, A. R. *J. Am. Chem. Soc.* **1953**, *75*, 2404.

(20) Klomp, D.; Maschmeyer, T.; Hanefeld, U.; Peters, J. A. *Chem.—Eur. J.* **2004**, *10*, 2088.

(21) Cohen, R.; Graves, C. R.; Nguyen, S. T.; Martin, J. L.; Ratner, M. A. *J. Am. Chem. Soc.* **2004**, *126*, 14796.

(22) Corma, A.; Domine, M. E.; Valencia, S. *J. Catal.* **2003**, *215*, 294.

(23) Renz, M.; Blasco, T.; Corma, A.; Fornés, V.; Jensen, R.; Nemeth, L. T. *Chem.—Eur. J.* **2002**, *8*, 4708.

(24) Corma, A.; Renz, M. *Chem. Commun.* **2004**, 550.

(25) Zhu, Y.; Chuah, G. K.; Jaenicke, S. *J. Catal.* **2004**, *227*, 1.

(26) Zhu, Y.; Yungtong, N.; Jaenicke, S.; Chuah, G. K. *J. Catal.* **2005**, *229*, 404.

(27) Boronat, M.; Concepción, P.; Corma, A.; Renz, M.; Valencia, S. *J. Catal.* **2005**, *234*, 111.

(28) Boronat, M.; Corma, A.; Renz, M.; Sastre, G.; Viruela, P. M. *Chem.—Eur. J.* **2005**, *11*, 6905.

(29) Newsam, J. M.; Treacy, M. M. J.; Koetsier, W. T.; de Gruyter, C. B. *Proc. R. Soc. London, A* **1988**, *420*, 375.

(30) Svensson, M.; Humbel, S.; Froese, R. D. J.; Matsubara, T.; Sieber, S.; Morokuma, K. *J. Phys. Chem.* **1996**, *100*, 19357.

(31) Humbel, S.; Sieber, S.; Morokuma, K. *J. Chem. Phys.* **1996**, *105*, 1959.

(32) Frisch, M. J.; et al. *Gaussian 03*, revision B.04; Gaussian, Inc.: Pittsburgh, PA, 2003.

(33) Perdew, J. P.; Wang, Y. *Phys. Rev. B* **1992**, *45*, 13244.

(34) Becke, A. D. *J. Chem. Phys.* **1993**, *98*, 5648.

(35) Hay, P. J.; Wadt, W. R. *J. Chem. Phys.* **1985**, *82*, 270.

(36) Wadt, W. R.; Hay, P. J. *J. Chem. Phys.* **1985**, *82*, 284.

(37) Hariharan, P. C.; Pople, J. A. *Theor. Chim. Acta* **1973**, *28*, 213.

(38) Solans-Monfort, X.; Sodupe, M.; Branchadell, V.; Sauer, J.; Orlando, R.; Ugliengo, P. *J. Phys. B* **2005**, *109*, 3539.

(39) Glendening, E. D.; Reed, A. E.; Carpenter, J. E.; Weinhold, F. *NBO*, version 3.1.

(40) Bare, S. R.; Kelly, S. D.; Sinkler, W.; Low, J. J.; Modica, F. S.; Valencia, S.; Corma, A.; Nemeth, L. *J. Am. Chem. Soc.* **2005**, *127*, 12924.

(41) Shetty, S.; Pal, S.; Kanhere, D. G.; Goursot, A. *Chem.—Eur. J.* **2006**, *12*, 518.